



Supplement of

Global estimates of ambient reactive nitrogen components during 2000–2100 based on the multi-stage model

Rui Li et al.

Correspondence to: Rui Li (rli@geo.ecnu.edu.cn) and Wenwen Sun (sunww@sumhs.edu.cn)

The copyright of individual parts of the supplement might differ from the article licence.

Three statistical indicators including determination coefficient (R^2), root mean square error (RMSE), and mean absolute error (MAE) were applied to validate the modelling performances of four N-bearing components (Li et al., 2019; Li et al., 2023). P_i and O_i represent the predicted and observed concentrations, respectively. SSR and SST represent the regression sum of squares and total sum of squares, respectively. The detailed equations are as follows:

$$R^2 = \frac{SSR}{SST} \quad (1)$$

$$RMSE = \sqrt{\frac{\sum_{i=1}^N (P_i - O_i)^2}{N}} \quad (2)$$

$$MAE = \frac{1}{N} \sum_{i=1}^N |P_i - O_i| \quad (3)$$

Besides, some redundant variables were also removed in the final model because it might degrade the predictive accuracy of the multi-stage model. The redundant variables include areas of snow/ice and tundra.

Table S1 The basic information and data sources of variables for N-bearing component estimates.

Dataset	Variable	Unit	Spatial resolution	Time resolution	Data source
N-bearing components	NO ₃ ⁻	µg/m ³	--	Monthly	NNDMN,
	HNO ₃	µg/m ³	--	Monthly	EANET,
	NH ₃	µg/m ³	--	Monthly	EMEP, and
	NH ₄ ⁺	µg/m ³	--	Monthly	CASTNET
NO ₂ tropospheric column	NO ₂ column	mole/cm ²	0.25°	Daily	NASA
NH ₃ column	NH ₃ column	mol/cm ²	0.5°	Daily	ISAI
Meteorology	D _{2m}	°C	0.25°	6-hour	
	T _{2m}	°C	0.25°	6-hour	
	U ₁₀	m/s	0.25°	6-hour	ERA-Interim
	V ₁₀	m/s	0.25°	6-hour	reanalysis
	BLH	m	0.25°	3-hour	product
	Sund	s	0.25°	6-hour	
	Sp	hPa	0.25°	6-hour	
	Tp	mm	0.25°	6-hour	
Land use types	Barren land	m ²	30 m	Annually	
	Grassland	m ²	30 m	Annually	
	Shrubland	m ²	30 m	Annually	Liu et al.
	Forest	m ²	30 m	Annually	(2020)
	Cropland	m ²	30 m	Annually	
	Tundra	m ²	30 m	Annually	
Elevation	Snow/ice	m ²	30 m	Annually	
	DEM	m	30 m	--	ETOPO

Table S2 Available (O) and not available (X) CMIP6 Global Climate Models used in our study.

	SSP1-2.6	SSP2-4.5	SSP3-7.0	SSP8.5
ACCESS-	O	O	O	O
ESM1-5				
CanESM5	O	O	O	O
CESM2-	O	O	O	O
WACCM				
CMCC-CM2-	O	O	O	O
SR5				
EC-Earth3-Veg	O	O	O	O
EC-Earth3-CC	X	O	X	O
FGOALS-f3-L	O	O	O	O
FGOALS-g	O	O	O	O
GFDL-ESM4	O	O	O	O
INM-CM5-0	O	O	O	O
IPSL-CM6A-LR	O	X	X	X
MIROC6	O	O	O	O
MPI-ESM1-2-	O	O	O	O
HR				
MRI-ESM2-0	O	O	O	O
Nor-ESM2-LM	O	O	O	O
NorESM2-MM	O	O	O	O

Table S3 The temporal variations of ambient HNO₃ concentrations (average concentrations) in many countries during 2000-2100.

Scenario	HNO ₃	China	India	Europe	United States	Brazil	Argentina	Democratic Congo	West Africa	Indonesia	South Korea
								Coast			
Historical	2000	0.25	0.37	0.23	0.20	0.32	0.13	0.33	0.31	0.40	0.36
	2005	0.34	0.45	0.26	0.22	0.32	0.14	0.36	0.35	0.41	0.56
	2010	0.39	0.52	0.26	0.20	0.33	0.15	0.36	0.35	0.43	0.56
	2013	0.42	0.50	0.25	0.19	0.32	0.15	0.37	0.31	0.41	0.60
	2015	0.34	0.50	0.26	0.19	0.32	0.15	0.38	0.32	0.41	0.52
	2019	0.35	0.54	0.25	0.17	0.33	0.15	0.38	0.35	0.42	0.51
SSP1-2.6	2020	0.25	0.50	0.18	0.08	0.26	0.07	0.34	0.28	0.30	0.35
	2040	0.12	0.39	0.11	0.05	0.24	0.05	0.32	0.25	0.21	0.24
	2060	0.07	0.31	0.08	0.03	0.20	0.04	0.32	0.24	0.16	0.18
	2080	0.06	0.27	0.06	0.03	0.16	0.03	0.30	0.22	0.09	0.15
	2100	0.05	0.24	0.05	0.03	0.13	0.03	0.30	0.19	0.06	0.14
SSP2-4.5	2020	0.28	0.55	0.18	0.08	0.29	0.08	0.32	0.22	0.34	0.37
	2040	0.18	0.48	0.15	0.06	0.26	0.06	0.30	0.22	0.22	0.26
	2060	0.12	0.40	0.14	0.05	0.24	0.05	0.27	0.23	0.14	0.22
	2080	0.08	0.38	0.13	0.05	0.22	0.04	0.25	0.20	0.10	0.18
	2100	0.07	0.35	0.11	0.05	0.18	0.03	0.21	0.17	0.08	0.17
SSP3-7.0	2020	0.32	0.60	0.20	0.09	0.37	0.09	0.33	0.32	0.38	0.46
	2040	0.36	0.55	0.20	0.07	0.32	0.10	0.36	0.34	0.43	0.50
	2060	0.32	0.49	0.21	0.07	0.27	0.11	0.39	0.37	0.38	0.45
	2080	0.26	0.45	0.20	0.07	0.25	0.13	0.44	0.39	0.31	0.35
	2100	0.24	0.41	0.17	0.06	0.22	0.13	0.40	0.39	0.29	0.29
SSP5-8.5	2020	0.27	0.58	0.20	0.10	0.30	0.09	0.32	0.24	0.32	0.38
	2040	0.25	0.52	0.18	0.09	0.28	0.10	0.27	0.24	0.30	0.29
	2060	0.23	0.45	0.19	0.10	0.25	0.10	0.26	0.26	0.28	0.28
	2080	0.17	0.42	0.19	0.12	0.22	0.09	0.25	0.26	0.20	0.21
	2100	0.11	0.38	0.17	0.12	0.20	0.05	0.26	0.31	0.13	0.19

Table S4 The temporal variations of ambient NH₃ concentrations (average concentrations) in many countries during 2000-2100.

Scenario	NH ₃	China	India	Europe	United States	Brazil	Argentina	Democratic Congo	West Africa	Indonesia	South Korea
Historical	2000	3.94	6.31	1.53	1.97	3.66	2.45	1.01	4.35	3.06	2.90
	2005	3.92	6.45	1.54	2.08	3.72	2.76	1.09	4.48	3.44	2.68
	2010	3.82	6.19	1.68	2.09	3.55	2.92	1.62	4.12	2.96	2.61
	2013	3.89	6.30	1.57	2.15	2.72	2.81	1.21	5.55	2.79	2.50
	2015	4.36	6.94	1.56	2.20	4.03	2.51	2.22	5.72	3.95	3.61
	2019	4.43	7.01	1.53	2.17	4.18	2.90	2.48	5.98	3.51	4.06
SSP1-2.6	2020	3.51	6.30	1.54	1.79	3.39	2.66	2.16	4.82	2.90	3.27
	2040	2.56	4.73	1.35	1.63	3.26	2.60	2.10	3.80	2.67	2.58
	2060	2.00	3.95	1.21	1.59	3.23	2.50	2.10	3.04	2.57	2.06
	2080	1.80	2.92	1.17	1.58	3.19	2.48	2.08	2.71	2.51	1.84
	2100	1.75	2.57	1.15	1.58	3.17	2.26	2.08	2.57	2.48	1.74
SSP2-4.5	2020	3.54	7.01	1.58	1.81	3.41	2.67	2.17	4.83	2.89	3.28
	2040	3.20	8.04	1.53	1.71	3.41	2.66	2.18	4.68	2.82	3.18
	2060	2.64	6.83	1.43	1.66	3.34	2.64	2.14	3.88	2.73	2.63
	2080	2.17	5.90	1.35	1.62	3.32	2.52	2.13	3.22	2.71	2.19
	2100	2.00	4.66	1.33	1.61	3.30	2.35	2.13	2.92	2.61	1.99
SSP3-7.0	2020	3.63	6.84	1.68	1.84	3.95	2.86	2.18	5.51	3.00	3.53
	2040	3.96	8.37	1.64	1.78	3.80	2.70	2.20	5.22	3.11	3.55
	2060	3.71	9.74	1.59	1.75	3.53	2.66	2.22	5.19	3.17	3.52
	2080	3.33	9.04	1.52	1.72	3.55	2.58	2.21	4.76	3.11	3.23
	2100	3.19	9.17	1.46	1.70	3.56	2.46	2.21	4.64	3.10	3.15
SSP5-8.5	2020	3.57	6.95	1.59	1.80	3.64	2.75	2.19	4.99	2.88	3.25
	2040	3.37	9.02	1.46	1.75	3.46	2.68	2.21	4.63	2.97	3.14
	2060	2.99	7.81	1.44	1.75	3.44	2.64	2.20	4.28	2.86	2.90
	2080	2.50	6.04	1.43	1.75	3.43	2.55	2.19	3.75	2.78	2.54
	2100	2.01	3.44	1.35	1.71	3.33	2.42	2.15	3.18	2.58	2.16

Table S5 The temporal variations of ambient NH₄⁺ concentrations (average concentrations) in many countries during 2000-2100.

Scenario	NH ₄ ⁺	China	India	Europe	United States	Brazil	Argentina	Democratic Congo	West Africa	Indonesia	South Korea
					States		Coast		Africa		Korea
Historical	2000	1.95	2.47	0.97	0.54	0.48	0.37	0.73	0.58	0.45	2.03
	2005	2.43	3.41	0.93	0.53	0.50	0.37	0.69	0.55	0.48	2.18
	2010	2.43	4.82	0.96	0.53	0.65	0.41	0.75	0.68	0.47	1.92
	2013	2.76	5.36	0.89	0.48	0.48	0.41	0.74	0.98	0.53	2.34
	2015	2.51	4.64	0.81	0.46	0.68	0.36	0.87	0.95	1.12	2.52
	2019	2.24	4.79	0.78	0.43	0.64	0.40	1.03	1.20	0.64	2.20
SSP1-2.6	2020	2.00	4.26	0.75	0.53	0.54	0.34	0.75	0.82	0.73	1.81
	2040	1.24	2.99	0.67	0.48	0.49	0.30	0.72	0.79	0.61	1.25
	2060	0.78	2.36	0.55	0.45	0.48	0.30	0.77	0.84	0.56	0.84
	2080	0.63	1.53	0.52	0.45	0.46	0.29	0.75	0.82	0.52	0.66
	2100	0.58	1.25	0.50	0.45	0.45	0.28	0.68	0.74	0.51	0.58
SSP2-4.5	2020	2.04	4.86	0.86	0.55	0.55	0.34	0.72	0.79	0.73	1.83
	2040	1.76	5.70	0.82	0.52	0.55	0.34	0.76	0.83	0.69	1.75
	2060	1.31	4.72	0.73	0.51	0.52	0.32	0.75	0.82	0.64	1.30
	2080	0.93	3.96	0.67	0.48	0.51	0.32	0.73	0.80	0.63	0.94
	2100	0.79	2.95	0.65	0.47	0.50	0.31	0.63	0.69	0.57	0.78
SSP3-7.0	2020	2.10	4.70	0.93	0.58	0.56	0.35	0.71	0.78	0.79	2.03
	2040	2.37	5.94	0.90	0.51	0.58	0.37	0.73	0.80	0.85	2.04
	2060	2.17	7.05	0.86	0.48	0.60	0.37	0.77	0.84	0.88	2.02
	2080	1.87	6.49	0.81	0.46	0.61	0.38	0.82	0.90	0.85	1.78
	2100	1.75	6.59	0.75	0.44	0.61	0.38	0.89	0.97	0.84	1.72
SSP5-8.5	2020	1.91	4.86	0.86	0.53	0.56	0.35	0.72	0.79	0.73	1.82
	2040	1.92	6.56	0.76	0.48	0.57	0.35	0.80	0.87	0.77	1.73
	2060	1.61	5.57	0.74	0.46	0.56	0.35	0.96	1.05	0.72	1.53
	2080	1.20	4.11	0.74	0.42	0.56	0.33	1.03	1.12	0.67	1.24
	2100	0.80	1.97	0.67	0.38	0.51	0.32	0.76	0.83	0.56	0.92

Figure S1 The spatial distribution of monitoring sites of reactive nitrogen components at the global scale. The color bar reflects the map of global terrain (altitude).

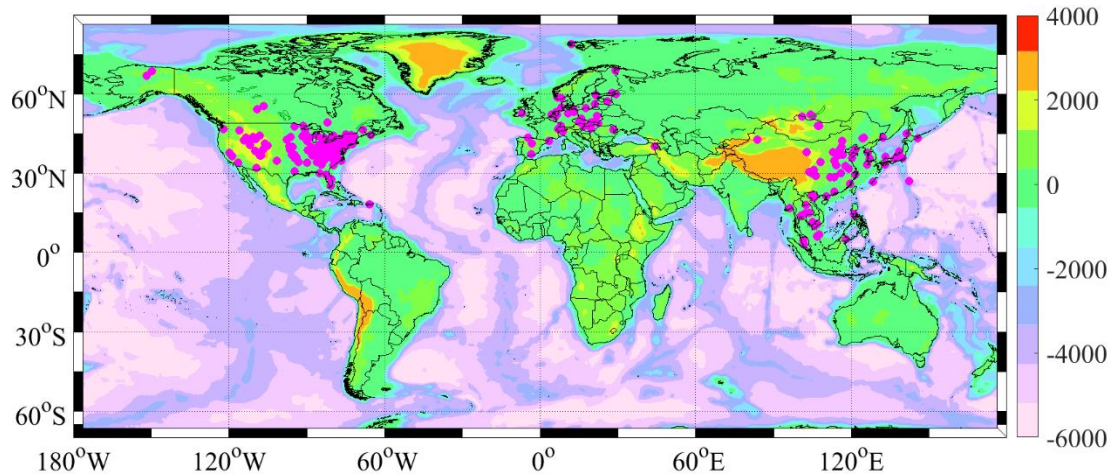


Figure S2 The predictive performances of four N-bearing components including NO_3^- (a), HNO_3 (b), NH_3 (c), and NH_4^+ (d) based on ensemble model. The model was constructed with 90% original data and the remained data was applied to validate the model. The black solid line denotes the best-fitting curve for all of the points, while the black dashed line represents the diagonal, which means the same observed and simulated values.

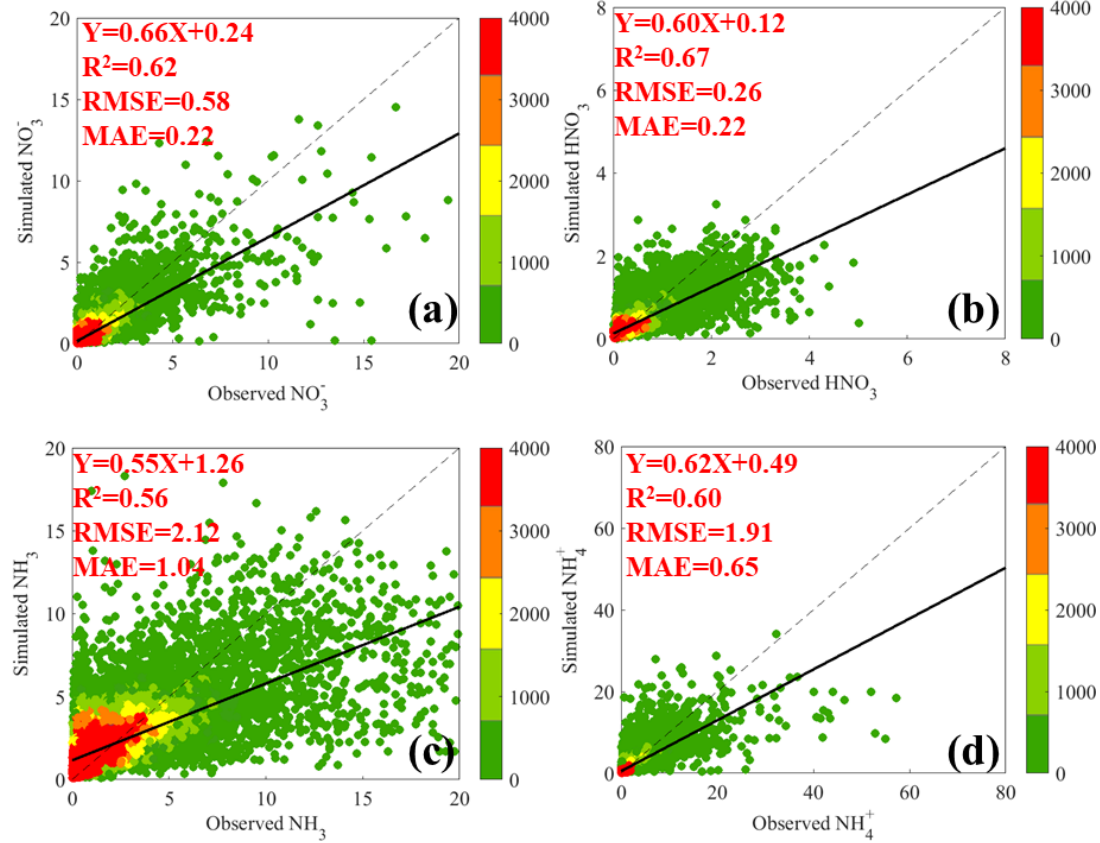


Figure S3 The annual mean concentrations of NO_3^- (a), HNO_3 (b), NH_3 (c), and NH_4^+ (d) at the global scale (Unit: $\mu\text{g N m}^{-3}$).

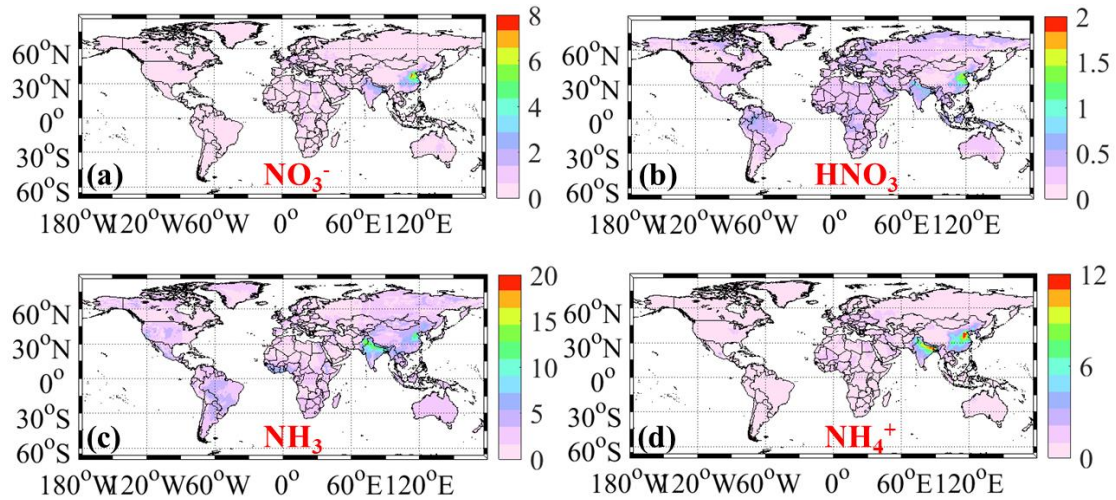


Figure S4 The seasonal variations of NO_3^- levels at the global scale (Unit: $\mu\text{g N m}^{-3}$).

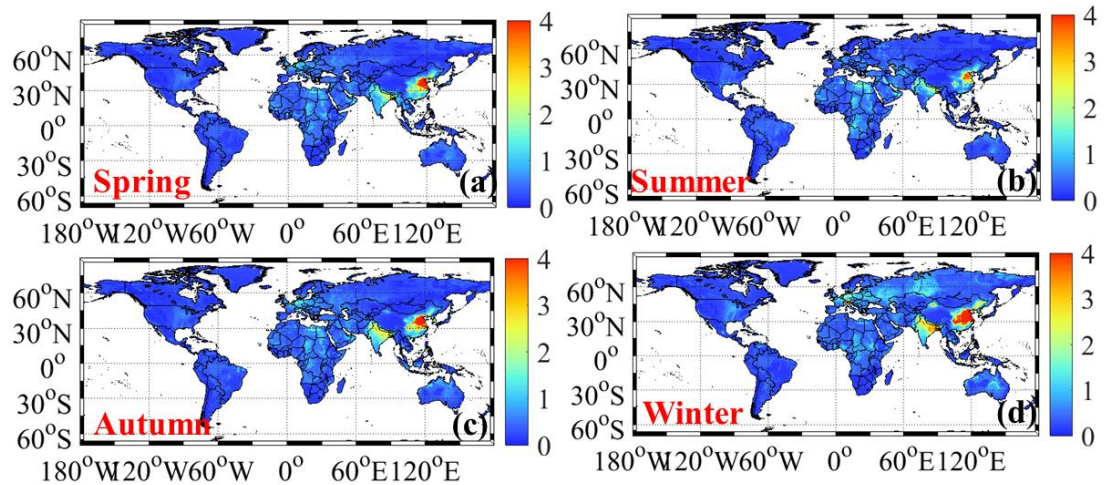


Figure S5 The seasonal variations of HNO₃ levels at the global scale (Unit: $\mu\text{g N m}^{-3}$).

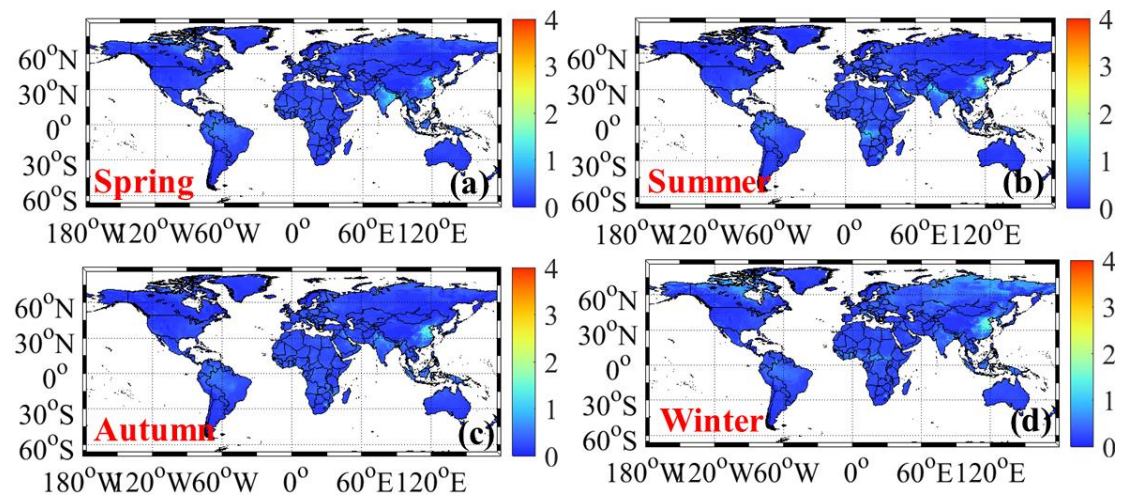


Figure S6 The seasonal variations of NH₃ levels at the global scale (Unit: $\mu\text{g N m}^{-3}$).

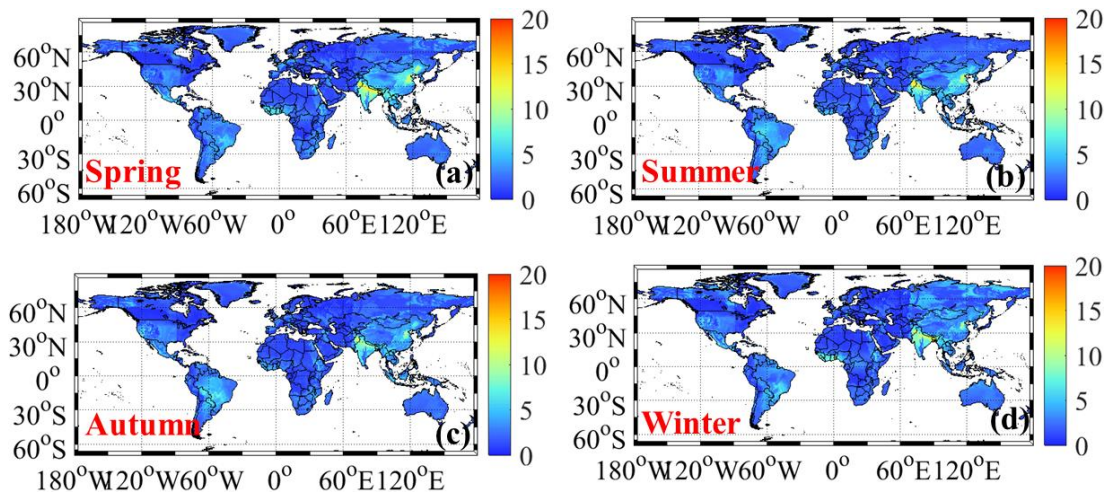


Figure S7 The seasonal variations of NH_4^+ levels at the global scale (Unit: $\mu\text{g N m}^{-3}$).

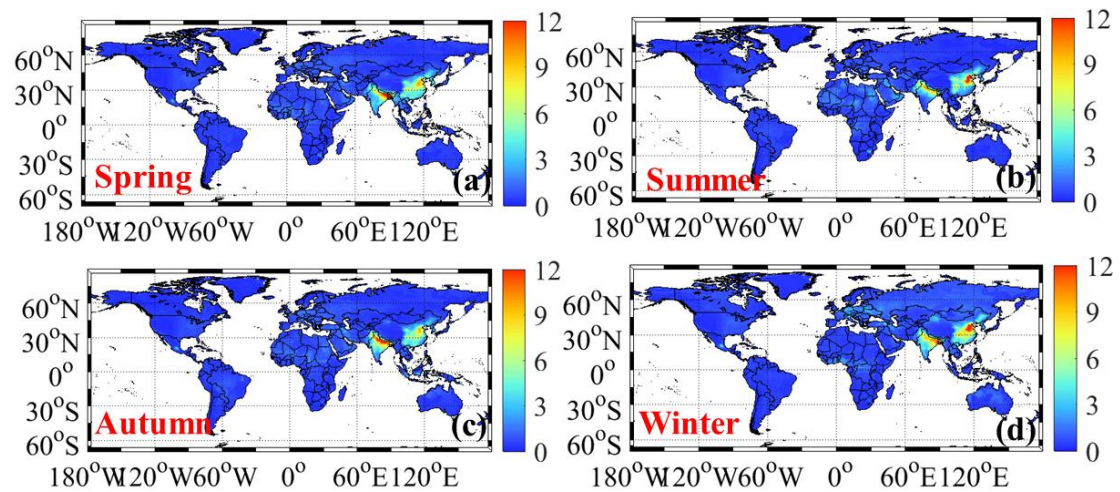


Figure S8 The monthly variations of NO_3^- , HNO_3 , NH_3 , and NH_4^+ in China, Europe, and the United States (Unit: $\mu\text{g N m}^{-3}$)

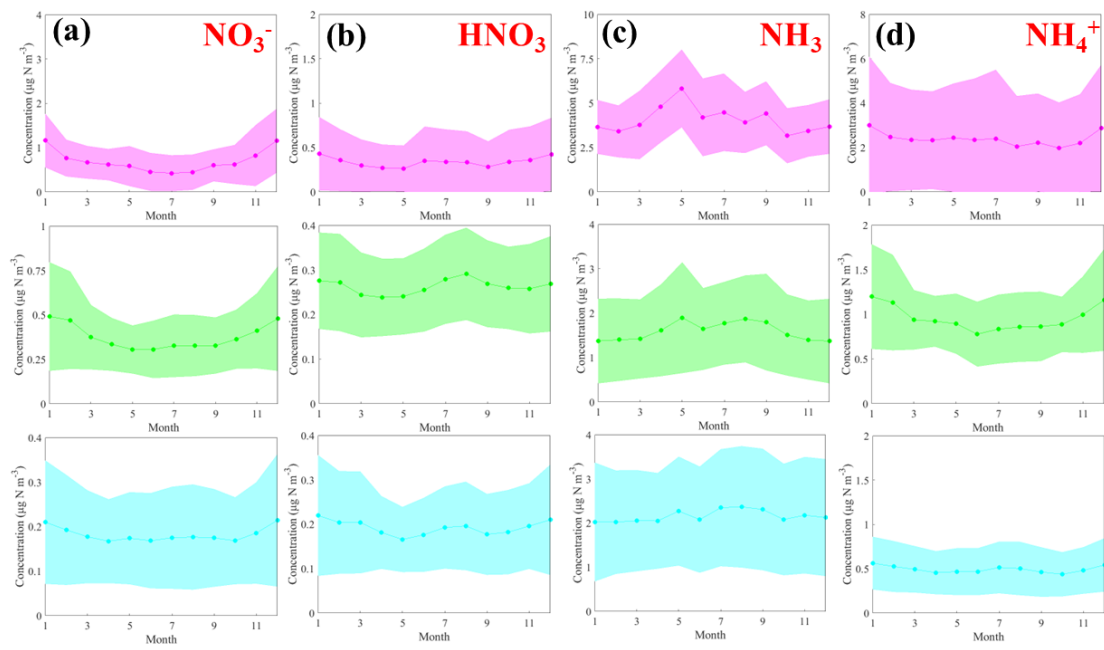


Figure S9 The yearly variations of NO_3^- (a), HNO_3 (b), NH_3 (c), and NH_4^+ (d) concentrations around the world during 2000-2019 (Unit: $\mu\text{g N m}^{-3}/\text{yr}$).

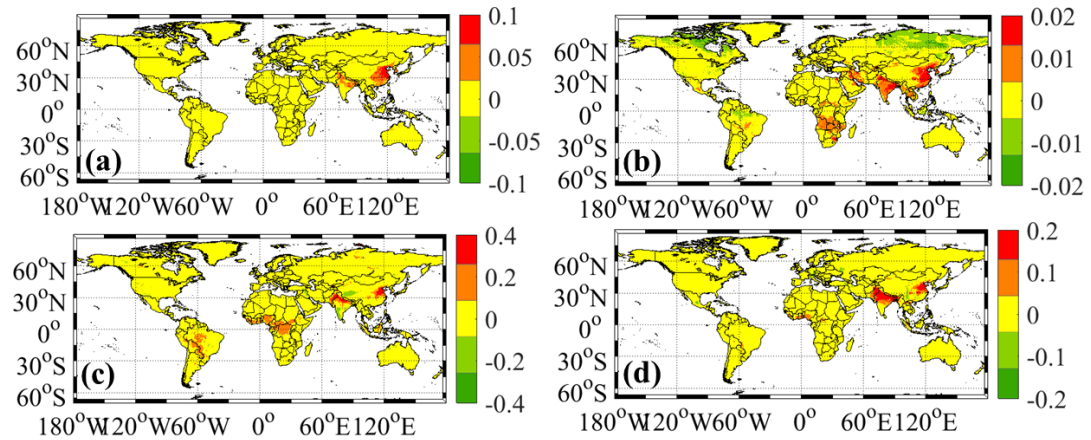


Figure S10 The yearly variations of NO_3^- (a), HNO_3 (b), NH_3 (c), and NH_4^+ (d) concentrations around the world during 2000-2007 (Unit: $\mu\text{g N m}^{-3}/\text{yr}$).

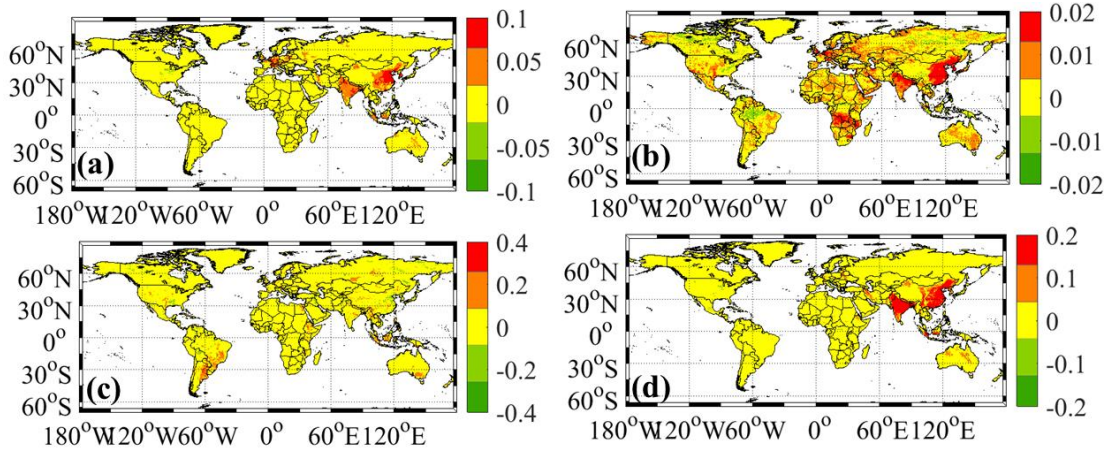


Figure S11 The yearly variations of NO_3^- (a), HNO_3 (b), NH_3 (c), and NH_4^+ (d) concentrations around the world during 2007-2013 (Unit: $\mu\text{g N m}^{-3}/\text{yr}$).

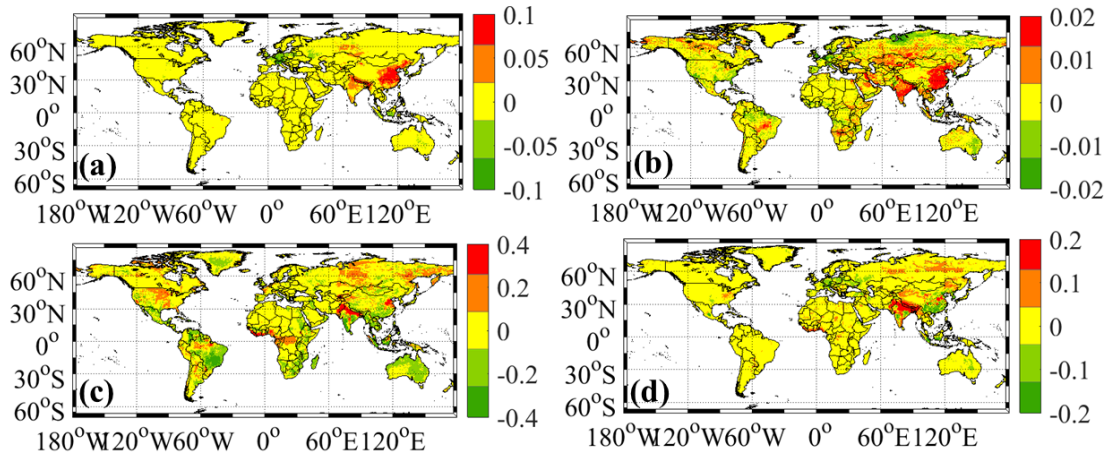


Figure S12 The yearly variations of NO_3^- (a), HNO_3 (b), NH_3 (c), and NH_4^+ (d) concentrations around the world during 2013-2019 (Unit: $\mu\text{g N m}^{-3}/\text{yr}$).

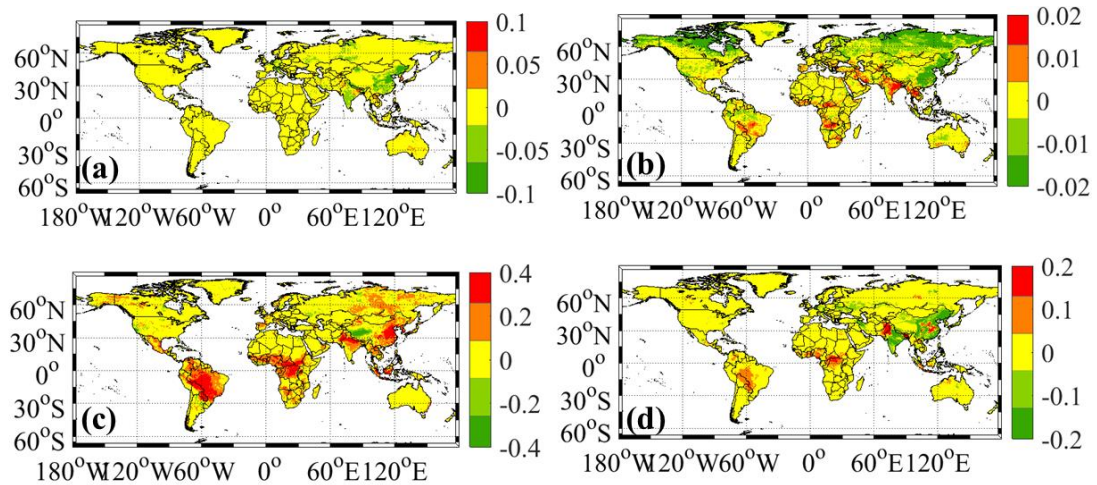


Figure S13 Spatial variations of projected global ambient concentrations of reactive nitrogen components under different climate change scenarios (Unit: $\mu\text{g N m}^{-3}$). Panels (a-b) represent the annual mean concentrations of ambient HNO_3 under SSP1-2.6, SSP2-4.5 during 2021-2100, respectively.

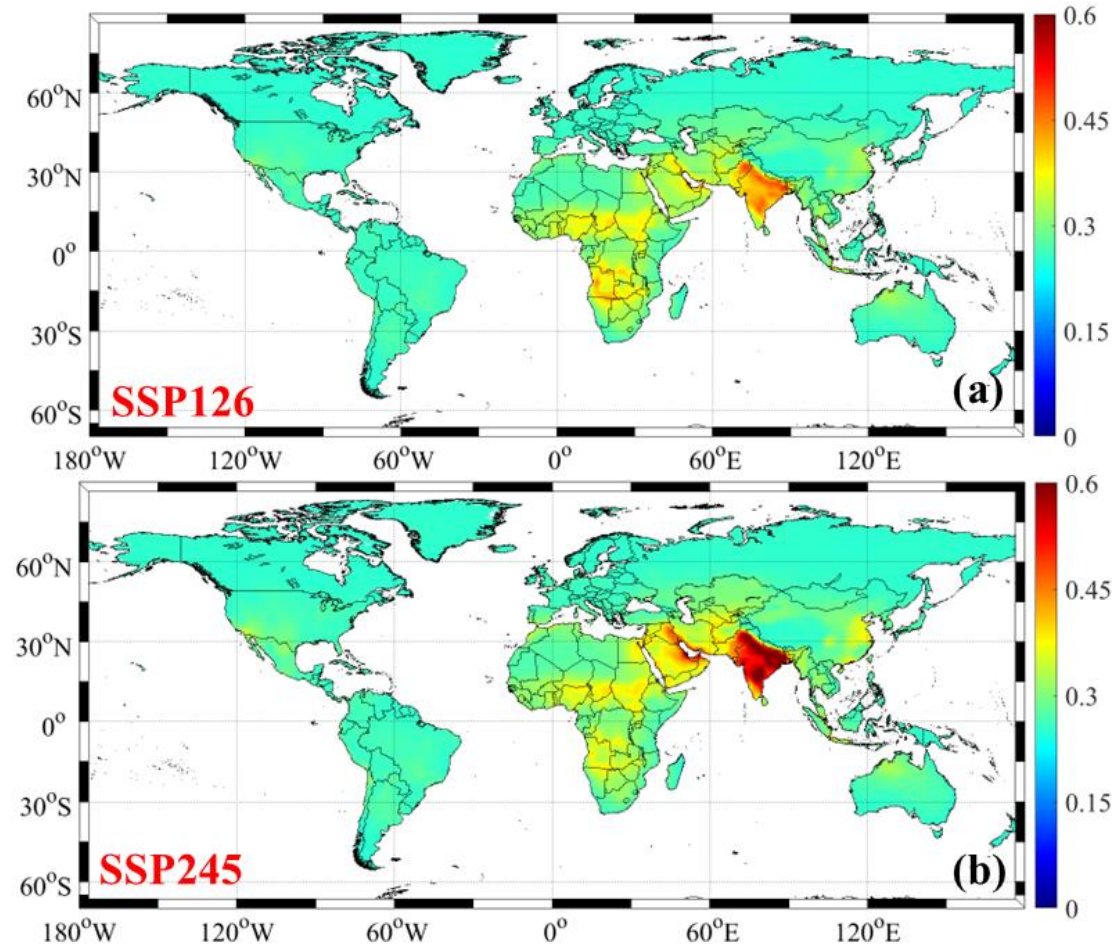


Figure S14 Spatial variations of projected global ambient concentrations of reactive nitrogen components under different climate change scenarios (Unit: $\mu\text{g N m}^{-3}$). Panels (a-b) represent the annual mean concentrations of ambient HNO_3 under SSP3-7.0, and SSP5-8.5 during 2021-2100, respectively.

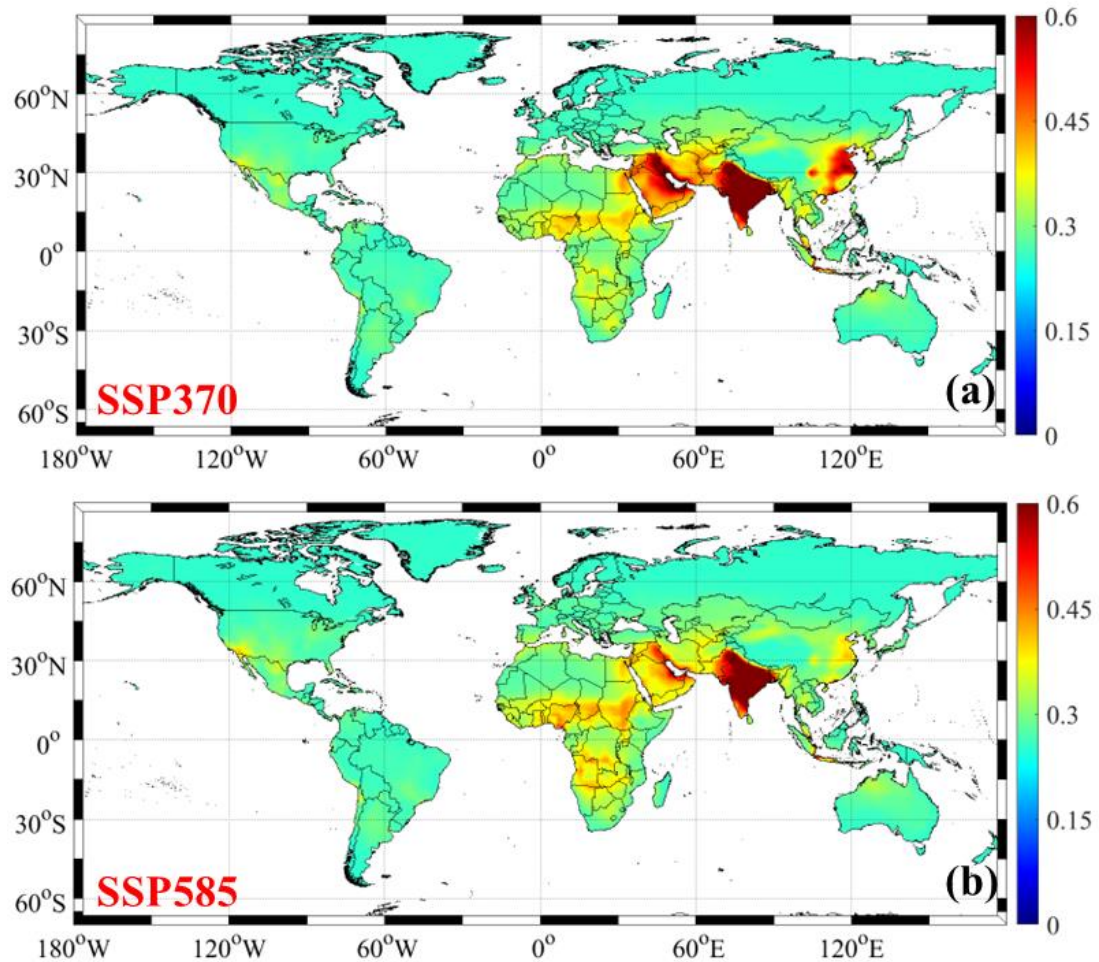


Figure S15 Spatial variations of projected global ambient concentrations of reactive nitrogen components under different climate change scenarios (Unit: $\mu\text{g N m}^{-3}$). Panels (a-b) represent the annual mean concentrations of ambient NH_3 under SSP1-2.6, SSP2-4.5 during 2021-2100, respectively.

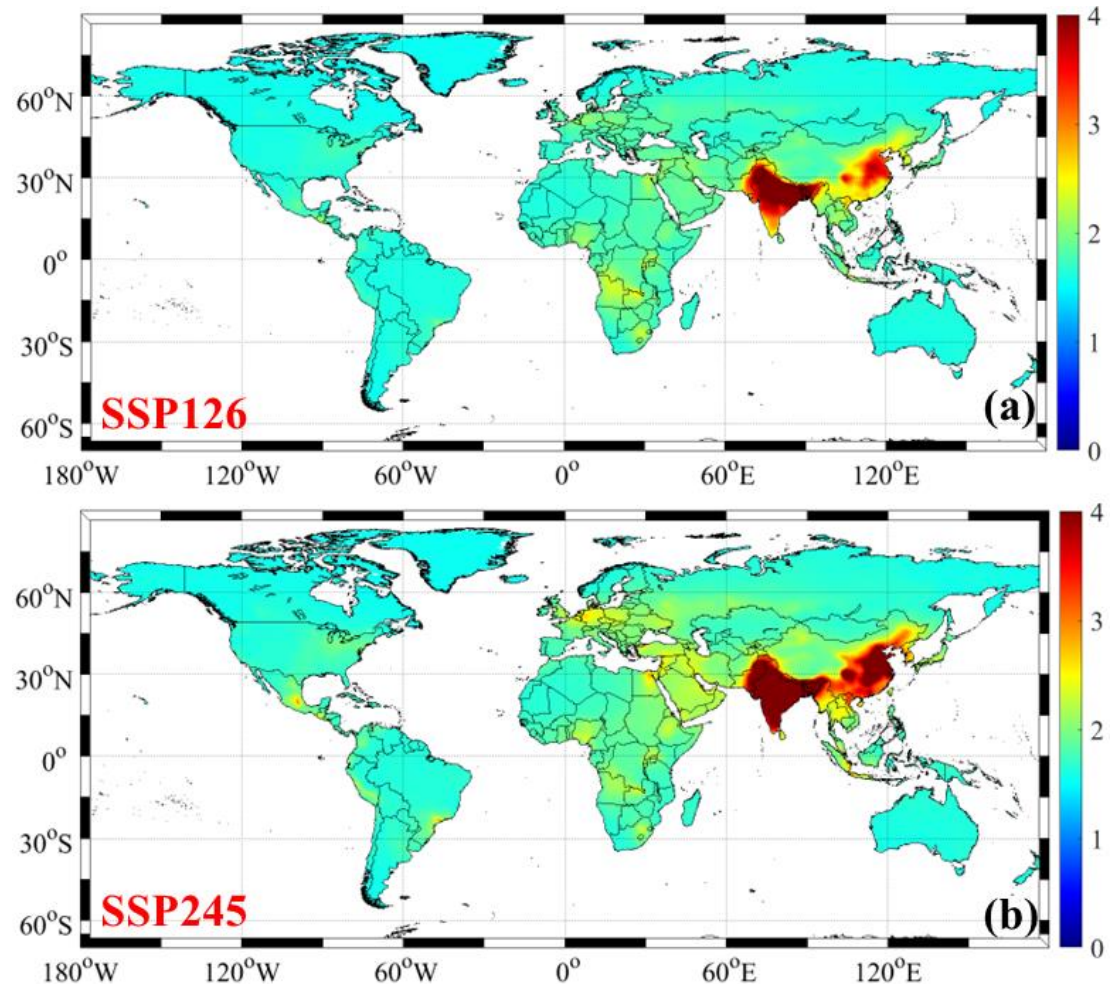


Figure S16 Spatial variations of projected global ambient concentrations of reactive nitrogen components under different climate change scenarios (Unit: $\mu\text{g N m}^{-3}$). Panels (a-b) represent the annual mean concentrations of ambient NH_3 under SSP3-7.0, and SSP5-8.5 during 2021-2100, respectively.

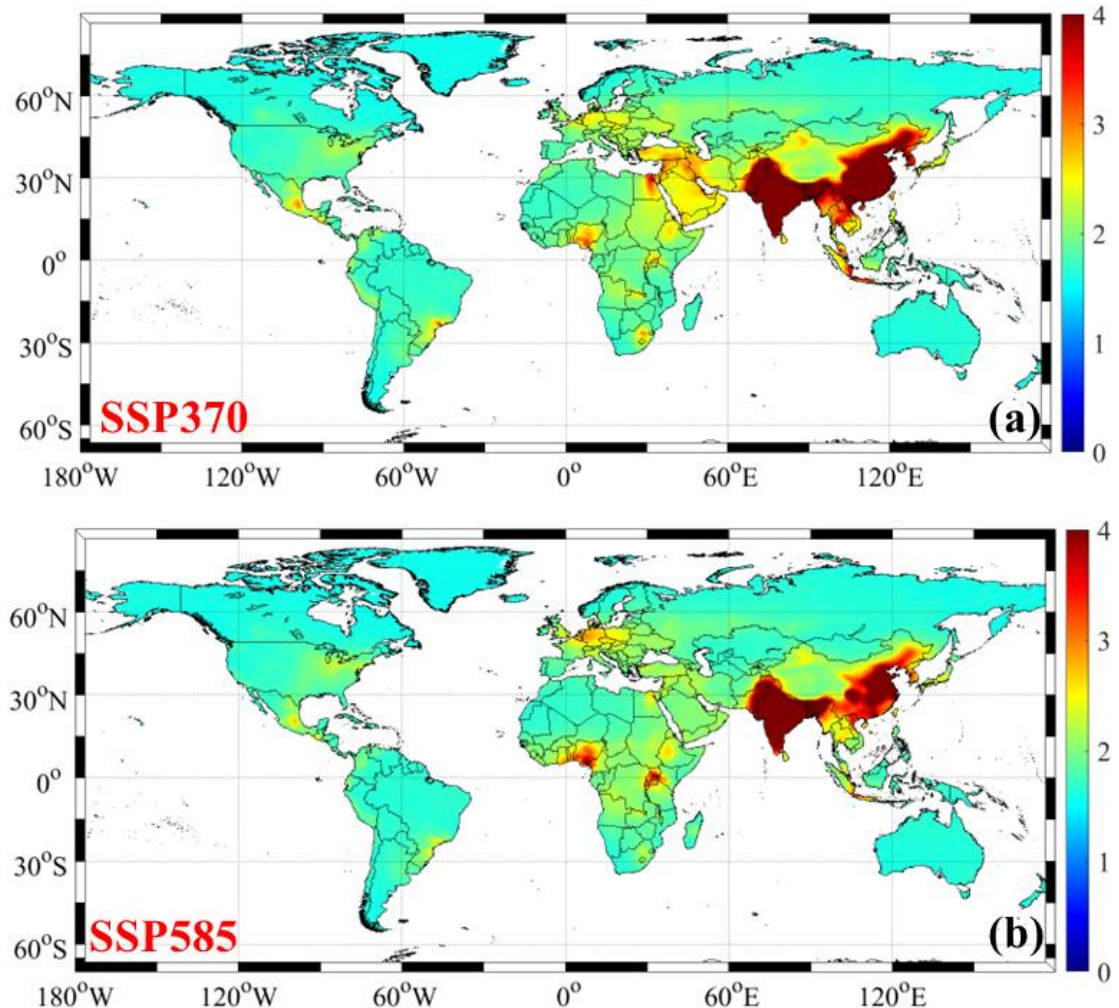


Figure S17 Spatial variations of projected global ambient concentrations of reactive nitrogen components under different climate change scenarios (Unit: $\mu\text{g N m}^{-3}$). Panels (a-b) represent the annual mean concentrations of ambient NH_4^+ ($\text{NH}_4\text{-N}$) under SSP1-2.6, SSP2-4.5 during 2021-2100, respectively.

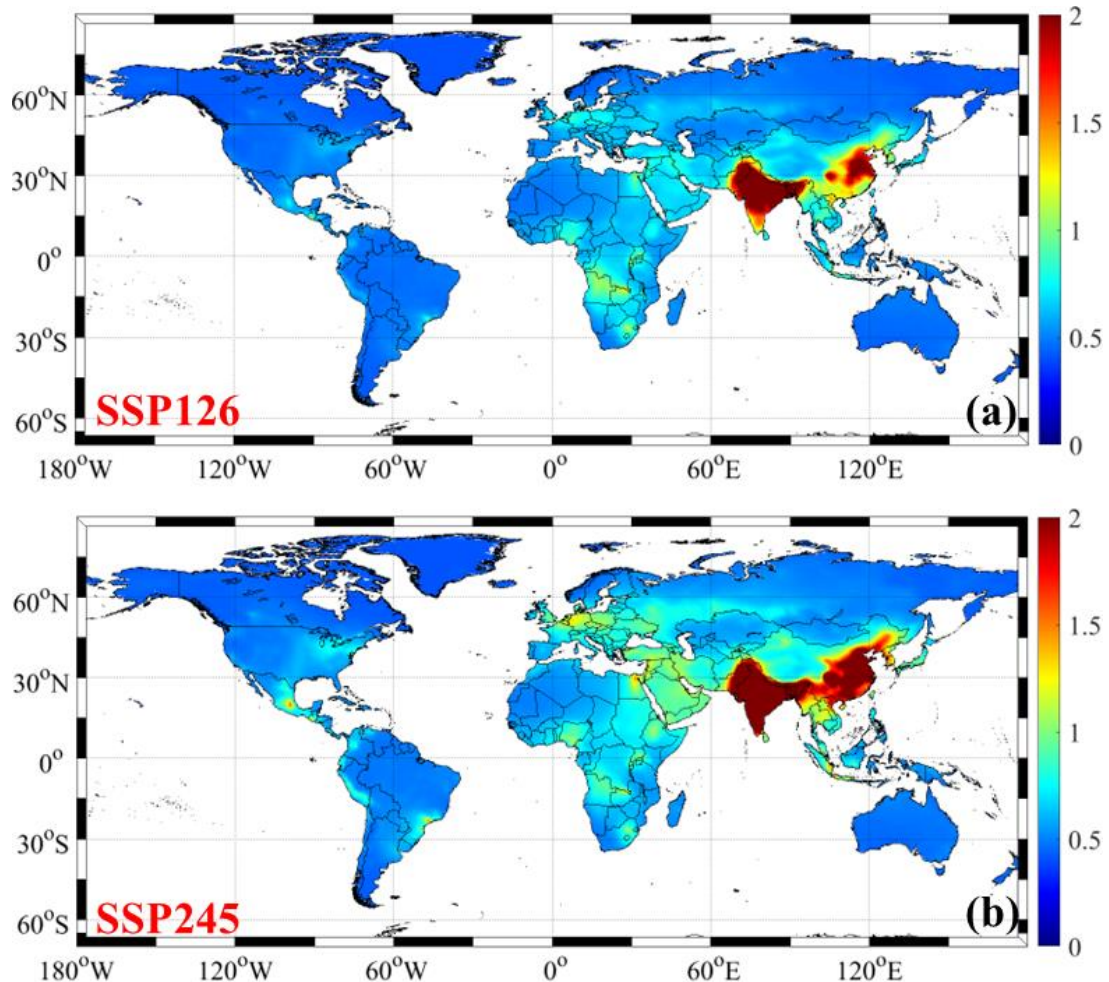
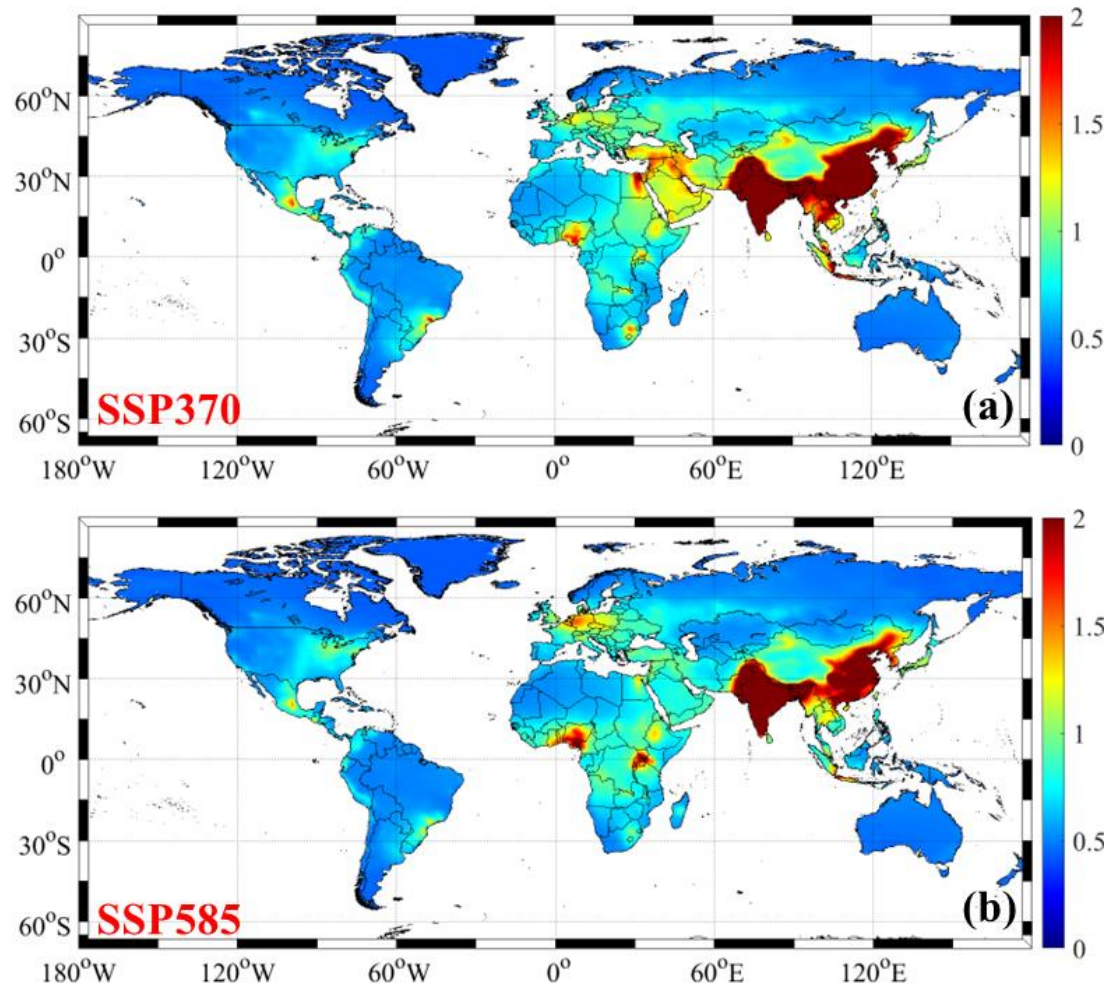


Figure S18 Spatial variations of projected global ambient concentrations of reactive nitrogen components under different climate change scenarios (Unit: $\mu\text{g N m}^{-3}$). Panels (a-b) represent the annual mean concentrations of ambient NH_4^+ ($\text{NH}_4\text{-N}$) under SSP3-7.0, and SSP5-8.5 during 2021-2100, respectively.



References

- Li, R., Gao, Y., Xu, J., Cui, L., Wang, G. (2023) Impact of Clean Air Policy on Criteria Air Pollutants and Health Risks Across China During 2013-2021. *Journal of Geophysical Research: Atmospheres* 128, e2023JD038939.
- Li, R., Cui, L., Zhao, Y., Zhang, Z., Sun, T., Li, J., Zhou, W., Meng, Y., Huang, K., Fu, H. (2019) Wet deposition of inorganic ions in 320 cities across China: spatio-temporal variation, source apportionment, and dominant factors. *Atmospheric Chemistry and Physics* 19, 11043-11070.